JACS
JOURNAL OF THE AMERICAN CHEMICAL SOCIETY

Communication

pubs.acs.org/JACS

# Hydrogen Activation and Metal Hydride Formation Trigger Cluster Formation from Supported Iridium Complexes

Jing Lu, Ceren Aydin, Nigel D. Browning,‡ and Bruce C. Gates*

Department of Chemical Engineering and Materials Science, University of California, One Shields Avenue, Davis, California 95616, United States

Supporting Information

**ABSTRACT:** The formation of iridium clusters from supported mononuclear iridium complexes in $H_2$ at 300 K and 1 bar was investigated by spectroscopy and atomic-resolution scanning transmission electron microscopy. The first steps of cluster formation from zeolite-supported $Ir(C_2H_4)_2$ complexes are triggered by the activation of $H_2$ and the formation of iridium hydride, accompanied by the breaking of iridium−support bonds. This reactivity can be controlled by the choice of ligands on the iridium, which include the support.

Oxide- and zeolite-supported metal complexes and clusters are important industrial catalysts,[1,2] and the interconversion[3] of these structures may dictate the catalyst performance.[4] Noble metals in isolated cationic complexes on supports[5] are easily reduced and aggregated, and a practical challenge is to control the metal oxidation state and degree of aggregation.[6]

$H_2$ is a widely used reactant in catalytic processes, exemplified by alkene hydrogenation,[7] hydrocarbon reforming,[8] hydrotreating,[9] and Fischer−Tropsch synthesis,[10] but it is also associated with metal reduction and aggregation[11,12] and the attendant loss of metal surface area. Extensive effort has been devoted to characterization of the processes of reduction and aggregation of supported metals, with insights into cluster formation having emerged from investigations of the kinetics.[13−15] $H_2$-induced formation of metal clusters from supported mononuclear metal complexes typically involves reduction, migration of metal species on the support surface, and metal−metal bond formation. There is lack of understanding of the first steps in the chemistry of cluster formation and of how the support and ligands on the metal influence the process.

Our goal was to characterize metal−$H_2$ interactions in supported iridium complexes and provide evidence of how they initiate iridium cluster formation. We chose iridium because it has a tendency to form small, stable clusters (e.g., $Ir_4$ and $Ir_6$) on various supports[16] and because it is a catalyst for hydrocarbon reactions such as hydrogenation,[17] dehydrogenation,[18] and naphthene ring opening.[19] We chose MgO and HY zeolite as the supports because they are stable porous materials with highly crystalline structures that lend themselves to examination by high-resolution scanning transmission electron microscopy (STEM) and offer contrasting ligand properties, with MgO being a much stronger electron donor than the zeolite.[20,21]

The results presented here show that $H_2$ dissociation on supported iridium complexes triggers cluster formation, and the reactivity for $H_2$ activation depends on both the support and the other ligands on the iridium. Moreover, $H_2$ activation is accompanied by the breaking of Ir−support bonds and thereby facilitates the migration of the iridium species leading to cluster formation.

MgO- and HY zeolite-supported $Ir(C_2H_4)_2$ complexes (zeolite Si/Al atomic ratio = 30) were synthesized by the reaction of $Ir(C_2H_4)_2(acac)$ (acac is acetylacetonate) with each support.[20] Zeolite-supported $Ir(C_2H_4)(CO)$ complexes were prepared by treatment of the supported $Ir(C_2H_4)_2$ with CO and $C_2H_4$.[20,22]

Infrared (IR) and extended X-ray absorption fine structure (EXAFS) spectra identified the supported species and showed that each was anchored to the support by two Ir−O bonds.[20] STEM images (Figure 1A−C) show the presence of only single Ir atoms on the supports and confirm that the initially prepared samples consisted of site-isolated mononuclear iridium complexes with no evidence of iridium clusters. The iridium complexes (Scheme 1) incorporated $\pi$-bonded ethene ligands,

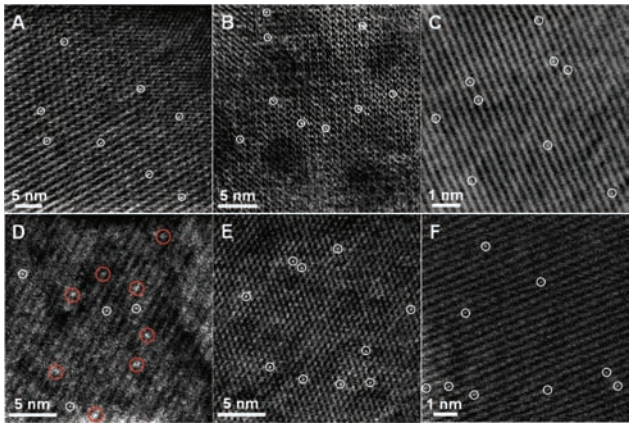


**Figure 1.** Aberration-corrected HAADF-STEM (*Z*−contrast) images characterizing the initially prepared samples (A−C) and samples after treatment in flowing $H_2$ at 300 K for 1 h (D−F), with the starting materials being $Ir(C_2H_4)_2$ on HY zeolite (A,D), $Ir(C_2H_4)(CO)$ on HY zeolite (B,E), and $Ir(C_2H_4)_2$ on MgO (C,F). The iridium species appear as bright features in the images. Some examples of isolated Ir atoms are circled in white and iridium clusters in red.

**Received:** December 5, 2011
**Published:** March 7, 2012

   dx.doi.org/10.1021/ja211380p | *J. Am. Chem. Soc.* 2012, 134, 5022−5025

**Scheme 1. Schematic Representations of the Structures of Supported Iridium Complexes**

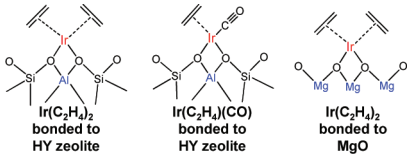


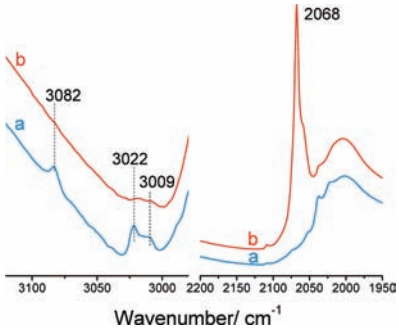


**Figure 2.** IR spectra (absorbance) in the $\nu_{CH}$ region (left) and $\nu_H/\nu_{CO}$ region (right) characterizing the HY zeolite-supported $Ir(C_2H_4)_2$ in (a) flowing helium and (b) after this sample had been in contact with flowing $H_2$ for 10 min at 300 K and 1 bar.

as evidenced by the $\nu_{CH}$ IR bands in the range of 3000–3100 $cm^{-1}$ (Figure 2 and Figure S1 in the Supporting Information).[23,24]

IR spectra characterizing the zeolite-supported $Ir(C_2H_4)_2$ after reaction with $H_2$ at 300 K show the immediate appearance of an Ir–H band at 2068 $cm^{-1}$ (Figure 2), assigned on the basis of comparisons with the spectra of crystallographically characterized complexes.[25] The frequency shifted to 1509 $cm^{-1}$ when the flowing $H_2$ was replaced by flowing $D_2$ (Figure S2), with the shift matching that expected for replacement of Ir–H by Ir–D.[26,27] The formation of iridium hydrides from zeolite-supported $Ir(C_2H_4)_2$ was accompanied by hydrogenation of $\pi$-bonded ethene ligands, demonstrated by IR spectra showing the rapid disappearance of the $C_2H_4$ bands at 3009, 3022, and 3082 $cm^{-1}$ (Figure 2) and the concomitant growing in of ethyl bands at 2876, 2936, and 2964 $cm^{-1}$ (Figure S3).[28]

In agreement with the IR data, EXAFS data characterizing the zeolite-supported $Ir(C_2H_4)_2$ show a decrease in the Ir–C coordination number (CN) from ~4 to ~2 after 15 min of contact with $H_2$, accompanied by the appearance of a contribution identified as a second Ir–C (Table S1) shell as ethene ligands were converted to ethyl.

In contrast to the Ir–H formation and hydrogenation of ethene ligands on zeolite-supported $Ir(C_2H_4)_2$, no iridium hydride formation from the zeolite-supported $Ir(C_2H_4)(CO)$ or MgO-supported $Ir(C_2H_4)_2$ occurred, as shown by the IR spectra (Figure S1)—the ethene ligands were stable in $H_2$.

To further examine the differences in metal–hydrogen interactions in the samples, the catalytic activity of each was determined for H–D exchange in the reaction of $H_2$ and $D_2$ in a once-through steady-state plug-flow reactor at 300 K and 1 bar. The concentration of HD in the effluent stream was measured with a mass spectrometer (Table 1). Neither the zeolite nor the MgO alone is active for the H–D exchange reaction. The catalytic activity of the sample initially consisting of zeolite-supported $Ir(C_2H_4)_2$ for H–D exchange was relatively high, with HD produced at an equilibrium concentration that could not be avoided under our conditions, either by decreasing the sample mass to the lowest that could be measured accurately or increasing the $H_2 + D_2$ flow rate to the maximum the system could handle.[29] In contrast, the conversions were 2–3 orders of magnitude lower when the catalyst was MgO-supported $Ir(C_2H_4)_2$ or zeolite-supported $Ir(C_2H_4)(CO)$ under the same conditions.

IR spectroscopy was used to characterize the samples working as catalysts in flowing $H_2 + D_2$ (Figure 3). The

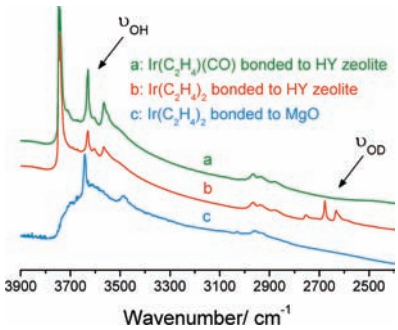


**Figure 3.** IR spectra (absorbance) in the $\nu_{OH}$ and $\nu_{OD}$ regions characterizing (a) $Ir(C_2H_4)(CO)$ on HY zeolite, (b) $Ir(C_2H_4)_2$ on HY zeolite, and (c) $Ir(C_2H_4)_2$ on MgO after treatment in flowing equimolar $H_2 + D_2$ for 5 min at 300 K and 1 bar.

bands indicative of support surface OH groups in the zeolite-supported sample initially incorporating $Ir(C_2H_4)_2$ shifted from 3566, 3630, and 3746 $cm^{-1}$ to 2633, 2678, and 2753 $cm^{-1}$ under the influence of $H_2 + D_2$. The new bands are assigned to zeolite surface OD groups, because the frequencies match the expected values as H is replaced by D according to the Hooke's law approximation.[26] This result demonstrates that after $D_2$ had been activated on the iridium complex, it migrated on the support and reacted with support OH groups to give OD groups—this is the well-known hydrogen spillover process.[30] Because no support OD groups formed from the zeolite-supported $Ir(C_2H_4)(CO)$ or MgO-supported $Ir(C_2H_4)_2$

**Table 1. Spectra and Catalytic Reaction Data Characterizing Metal–Hydrogen Interactions in Supported Iridium Complexes at 300 K and 1 bar**

| initial form of complex/support | $N_{Ir-Ir}$ after $H_2$ treatment for 1 h[a] | activity for $H_2/D_2$ exchange (% conversion relative to equilibrium)[b] | IR spectroscopic evidence of Ir–H bonds in complex after reaction with $H_2$? | reactivity of ethene ligands in $H_2$ |
|---|---|---|---|---|
| $Ir(C_2H_4)_2$/HY zeolite | 1.3 | 100 | yes | rapid conversion to ethyl |
| $Ir(C_2H_4)(CO)$/HY zeolite | 0 | 0.12 | no | none |
| $Ir(C_2H_4)_2$/MgO | 0 | 1.1 | no | none |

[a]Coordination number determined by EXAFS spectroscopy (details of EXAFS results shown in Table S1). [b]The error bound (standard deviation) is estimated to be ±1%.


dx.doi.org/10.1021/ja211380p | J. Am. Chem. Soc. 2012, 134, 5022–5025

complexes under the same conditions, we infer that the latter complexes did not activate $H_2$ or $D_2$, consistent with the results stated above.

In summary, the IR spectra demonstrate iridium hydride formation when the zeolite-supported $Ir(C_2H_4)_2$ groups react with $H_2$, and the $H_2$ activation is confirmed by hydrogen spillover and by the rapid reaction of $H_2$ with $D_2$ catalyzed by the complex formed from $Ir(C_2H_4)_2$. No such activation of $H_2$ was observed for the other two samples.

The activation of $H_2$ by the zeolite-supported $Ir(C_2H_4)_2$ is associated with the destabilization of iridium−support-oxygen bonds, as indicated by the transient EXAFS data (Figures 4 and

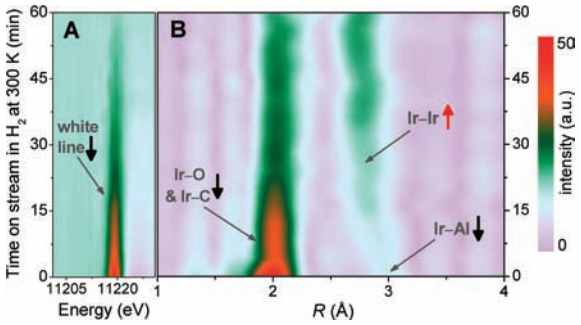


**Figure 4.** Transient data showing changes in the sample initially incorporating $Ir(C_2H_4)_2$ supported on HY zeolite during cluster formation in $H_2$ over a period of 60 min: (A) Ir $L_{III}$-edge XANES spectra and (B) the $k^3$-weighted Fourier-transformed EXAFS data recorded in 3-min intervals. The arrows show the directions of the changes.

S4), which demonstrate immediate decreases in the magnitude of the Ir−backscatterer contributions at short distances (~2.0 Å, assigned to Ir−$O_{support}$ and Ir−C), as well as of a weaker contribution at ~3.0 Å assigned to Ir−Al. Specifically, the average CN values characterizing the Ir−$O_{support}$ and Ir−Al contributions decreased from 2.0 to 1.2 and from 1.0 to 0.7, respectively, after 15 min of reaction with $H_2$ (Table S1).

In contrast, no changes in the Ir−$O_{support}$, Ir−Al, and Ir−Mg contributions were indicated by the EXAFS data characterizing the other two samples under the same conditions (Table S1).

Consistent with the H−D exchange and IR results, X-ray absorption near edge structure (XANES) spectra (Figures 4 and S4) characterizing the changes in the sample initially consisting of the zeolite-supported $Ir(C_2H_4)_2$ show a clear decrease in the Ir $L_{III}$-edge white line intensity, indicating a reduction of the iridium by $H_2$,[31] but there were no substantial changes in the Ir $L_{III}$-edge white lines characterizing the other samples (Figure S5). These data confirm the reactivity of the zeolite-supported $Ir(C_2H_4)_2$ complexes and the lack of reactivity of the other two with $H_2$ under these conditions.

The reduction indicated by the XANES data was accompanied by iridium cluster formation, as shown by the time-resolved EXAFS spectra recorded as the samples were treated in flowing $H_2$ at 300 K and 1 bar (Figure 4). The data characterizing the zeolite-supported $Ir(C_2H_4)_2$ demonstrate a rapid decrease in the magnitudes of the Ir−$O_{support}$, Ir−C, and Ir−Al contributions, demonstrating the unlinking of the iridium complex from the support and changes in the ligand environment of the iridium. The changes in these contributions were accompanied by the appearance and growth of a peak at ~2.7 Å, a typical Ir−Ir bonding distance,[31] indicating cluster formation. A detailed analysis of the EXAFS data recorded after 1 h of $H_2$ treatment confirmed the qualitative observations based on the Fourier-transformed EXAFS spectra (Tables 1 and S1), demonstrating the cluster formation (indicated by the Ir−Ir contribution, with a CN of 1.3) and the concomitant decrease of the CN characterizing the Ir−O contribution (from 2.0 to ~0.7), the Ir−C contribution (from 4.0 to ~1.1), and the Ir−Al contribution (from 1.0 to ~0.5).

In contrast, EXAFS spectra characterizing the other two samples after the same $H_2$ treatment showed neither detectable Ir−Ir contributions nor significant changes in the Ir−O, Ir−C, Ir−Al, and Ir−Mg contributions (Table S1).

Taken together, the XANES and EXAFS spectra demonstrate the reductive nature of the cluster formation from the zeolite-supported $Ir(C_2H_4)_2$.[32]

These results were complemented by STEM images showing atomically resolved iridium. Images were recorded for the initially prepared samples (Figure 1A−C), confirming that they initially incorporated iridium only in site-isolated complexes. Each of these samples was imaged after treatment in $H_2$ at 300 K and 1 bar for 1 h (Figure 1D−F; see Figure S6 for images recorded at lower magnifications). The image of Figure 1D confirms the EXAFS results, demonstrating that the reaction of the zeolite-supported $Ir(C_2H_4)_2$ with $H_2$ led to the formation of iridium clusters consisting of only a few atoms each, present with unconverted isolated iridium complexes. Thus, the images depict the initial steps of iridium cluster formation.

As expected, the images in Figure 1E,F demonstrate the absence of any iridium clusters and give evidence of only isolated mononuclear iridium complexes in the other two samples—consistent with the EXAFS results.

Thus, both the spectra and the images demonstrate that the zeolite-supported $Ir(C_2H_4)_2$ complexes react readily with $H_2$ accompanied by delinking of the iridium from the support and migration, reduction, and cluster formation at 300 K and 1 bar. In contrast, these changes did not occur when the complexes were zeolite-supported $Ir(C_2H_4)(CO)$ or MgO-supported $Ir(C_2H_4)_2$ under these conditions. To our knowledge, this is the first example illustrating the initial steps in the chemistry of $H_2$-induced cluster formation from supported metal complexes and evidence of how to control it.

Our IR spectra provide evidence of hydride ligands on the clusters formed from the zeolite-supported $Ir(C_2H_4)_2$. The presence of hydride ligands on the clusters was expected—such ligands on supported $Ir_4$ and $Ir_6$ clusters were predicted on the basis of theory to be highly stable.[33−35] The IR spectra demonstrate an increasing intensity of a band centered at 2068 $cm^{-1}$ characterizing Ir−H species as clusters formed during the $H_2$ treatment; this band is broader than that characterizing the mononuclear iridium hydride (Figure 2) and shifted slightly as the clusters grew (Figure S7).

Our results show that the tendency of a supported iridium complex to form clusters in the presence of $H_2$ is determined by the reactivity of the complex for formation of iridium hydrides. This pattern is consistent with observations showing that formation of metal hydride intermediates precedes the conversion in $H_2$ of metal ions in solution into metal clusters.[36]

Investigations by Finke et al.[13,14] of the kinetics of cluster formation from supported metal complexes in contact with a liquid (acetone or cyclohexane) indicate that the nucleation to form small clusters (seeds for the growth of larger particles) is rate-limiting under their conditions. Because both liquid-phase and surface reactions evidently play a role in the chemistry, the first steps of cluster formation under those conditions remain to


dx.doi.org/10.1021/ja211380p | J. Am. Chem. Soc. 2012, 134, 5022−5025

be clarified. Our data, obtained without the intervention of solution chemistry,[37] are in broad agreement with Finke's observations but indicate that formation of metal hydride intermediates can be rate limiting and that cluster formation can be controlled by the ligands on the metal, which include the support. Thus, a catalyst support may be selected not only to tune the catalytic activity and selectivity of a metal complex or cluster,[38,39] but also to control the resistance of the catalyst to deactivation by aggregation of the metal into (larger) clusters and particles.[40]

## ■ ASSOCIATED CONTENT

### Supporting Information

Detailed descriptions of the experimental methods, as well as additional images and spectra. This material is available free of charge via the Internet at http://pubs.acs.org.

## ■ AUTHOR INFORMATION


### Corresponding Author

bcgates@ucdavis.edu

### Present Address

‡Pacific Northwest National Laboratory, 902 Battelle Blvd., Richland, WA 99352


### Notes

The authors declare no competing financial interest.

## ■ ACKNOWLEDGMENTS

The work was supported by DOE Grants DE-SC0005822 (J.L.) and DE-FG02-03ER46057 (C.A.) and the University of California Lab Fee Program. We acknowledge beam time and support of the DOE Division of Materials Sciences for its role in the operation and development of beamline MR-CAT at Argonne National Laboratory and beamline 4-1 at the Stanford Synchrotron Radiation Lightsource.

## ■ REFERENCES


(1) Huber, G. W.; Iborra, S.; Corma, A. *Chem. Rev.* **2006**, *106*, 4044.
(2) De Vos, D. E.; Dams, M.; Sels, B. F.; Jacobs, P. A. *Chem. Rev.* **2002**, *102*, 3615.
(3) Serna, P.; Gates, B. C. *J. Am. Chem. Soc.* **2011**, *133*, 4714.
(4) Bell, A. T. *Science* **2003**, *299*, 1688.
(5) Hlatky, G. G. *Chem. Rev.* **2000**, *100*, 1347.
(6) Newton, M. A. *Chem. Soc. Rev.* **2008**, *37*, 2644.
(7) Watzky, M. A.; Finke, R. G. *J. Am. Chem. Soc.* **1997**, *119*, 10382.
(8) Zaera, F. *Appl. Catal., A* **2002**, *229*, 75.
(9) Topsøe, H.; Clausen, B. S.; Massoth, F. E. In *Hydrotreating Catalysis Science and Technology*; Anderson, J. R., Boudart, M., Eds.; Springer: Berlin/New York, 1996.
(10) Paál, Z.; Menon, P. G. *Catal. Rev.* **1983**, *25*, 229.
(11) Wanke, S. E.; Flynn, P. C. *Catal. Rev.* **1975**, *12*, 93.
(12) Hughes, R. *Deactivation of Catalysts*; Academic Press: London, 1984.
(13) Watzky, M. A.; Finney, E. E.; Finke, R. G. *J. Am. Chem. Soc.* **2008**, *130*, 11959.
(14) Mondloch, J. E.; Wang, Q.; Frankel, A. I.; Finke, R. G. *J. Am. Chem. Soc.* **2010**, *132*, 9701.
(15) Chupas, P. J.; Chapman, K. W.; Jennings, G.; Lee, P. L.; Grey, C. P. *J. Am. Chem. Soc.* **2007**, *129*, 13822.
(16) Uzun, A.; Dixon, D. A.; Gates, B. C. *ChemCatChem* **2011**, 3, 95.
(17) Crabtree, R. H. *Top. Organomet. Chem.* **2011**, *34*, 1.
(18) Choi, J.; MacArthur, A. H. R.; Brookhart, M.; Goldman, A. S. *Chem. Rev.* **2011**, *111*, 1761.
(19) McVicker, G. B.; Daage, M.; Touvelle, M. S.; Hudson, C. W.; Klein, D. P.; Baird, W. C.; Cook., B. R.; Chen, J. G.; Hantzer, S.; Vaughan, D. E. W.; Ellis, E. S.; Feeley, O. C. *J. Catal.* **2002**, *210*, 137.
(20) Lu, J.; Serna, P.; Gates, B. C. *ACS Catal.* **2011**, *1*, 1549.
(21) Smith, A. K.; Hugues, F.; Theolier, A.; Basset, J.-M.; Ugo, R.; Zanderighi, G. M.; Bilhou, J. L.; Bilhou-Bougnol, V.; Graydon, W. F. *Inorg. Chem.* **1979**, *18*, 3104.
(22) On the basis of the peak areas in the IR spectra, we infer that the sample resulting from this treatment contained ~80% $Ir(C_2H_4)(CO)$ and ~20% $Ir(CO)_2$. Details of the characterizations are presented elsewhere.[20]
(23) Bent, B. E.; Mate, C. M.; Kao, C.-T.; Slavin, A. J.; Somorjai, G. A. *J. Phys. Chem.* **1988**, *92*, 4720.
(24) Uzun, A.; Bhirud, V. A.; Kletnieks, P. W.; Haw, J. F.; Gates, B. C. *J. Phys. Chem. C* **2007**, *111*, 15064.
(25) Oldham, W. J.; Hinkle, A. S.; Heinekey, D. M. *J. Am. Chem. Soc.* **1997**, *119*, 11028.
(26) Hadjiivanov, K. I.; Vayssilov, G. N. *Adv. Catal.* **2002**, *47*, 308.
(27) Empsall, H. D.; Hyde, E. M.; Mentzer, E.; Shaw, B. L.; Uttley, M. F. *J. Chem. Soc., Dalton Trans.* **1976**, 2069.
(28) Newell, H. E.; McCoustra, M. R. S.; Chesters, M. A.; De La Cruz, C. *J. Chem. Soc., Faraday Trans.* **1998**, *94*, 3695.
(29) Although we did not quantify the rate of the H−D exchange under these conditions, we did quantify the rate of the catalytic hydrogenation of ethene, which is characterized by a turnover frequency (defined as the number of molecules converted (Ir atom × s)$^{-1}$) with the sample initially in the form of the zeolite-supported $Ir(C_2H_4)_2$ when $C_2H_4$ was co-fed with $H_2$ ($C_2H_4$:$H_2$ molar ratio = 1:2); the value was found to be 0.69 $s^{-1}$.[19]
(30) Conner, W. C.; Falconer, J. L. *Chem. Rev.* **1995**, *95*, 759.
(31) Uzun, A.; Gates, B. C. *Angew. Chem., Int. Ed.* **2008**, *47*, 9245.
(32) One might suggest that the initial reaction between the supported $Ir(C_2H_4)_2$ complex and $H_2$ might be an oxidative addition, but there were too many changes in the ligand sphere of the iridium to allow elucidation of the elementary steps.
(33) Rösch, N.; Petrova, G. P.; Petkov, P. S.; Genest, A.; Krüger, S.; Aleksandrov, H. A.; Vayssilov, G. N. *Top. Catal.* **2011**, *54*, 363.
(34) Petkov, P. S.; Petrova, G. P.; Vayssilov, G. N.; Rösch, N. *J. Phys. Chem. C* **2010**, *114*, 8500.
(35) Petrova, G. P.; Vayssilov, G. N.; Rösch, N. *Phys. Chem. Chem. Phys.* **2010**, *12*, 11015.
(36) Halpern, J.; Czapski, J.; Jortner, J.; Stein, G. *Nature* **1960**, *186*, 629.
(37) Mondloch, J. E.; Finke, R. G. *J. Am. Chem. Soc.* **2011**, *133*, 7744.
(38) Stair, P. C. *Nat. Chem.* **2011**, *3*, 345.
(39) Tauster, S. J.; Fung, S. C.; Baker, R. T. K.; Horsley, J. A. *Science* **1981**, *211*, 1121.
(40) Nishihata, Y.; Mizuki, J.; Akao, T.; Tanaka, H.; Uenishi, M.; Kimura, M.; Okamoto, T.; Hamada, N. *Nature* **2002**, *418*, 164.